

ORIGINAL ARTICLE

Open Access



Active Profiling and Polishing Model and Validation Based on Rotor Spiral Groove

Guo Yu¹, Feng Li^{2*} , Yong-Min Yu³ and Shou-Xiang Zai⁴

Abstract

When a spiral groove is formed using superplastic molding, precision casting, additive manufacturing, or other non-mechanical processing technology, it is difficult to meet the molding precision required for direct use, and the surface quality and accuracy of the shape need to be improved through a finishing process. In view of the poor reachability of the current tool-based polishing process, a tool-less polishing method using free-abrasive grains for complex spiral grooves is proposed. With this method, by controlling the movement of the workpiece, the design basis and relative motion of the abrasive particles along a helical path remain consistent, resulting in a better polishing profile. A spiral groove of a revolving body is taken as the research object; the influence of the installation method and the position of the parts, as well as the effect of the rotational speed of the abrasive ball on its relative motion along a helical trajectory, are studied, and the polishing cutting process of an abrasive ball is reasonably simplified. A consistent mathematical model of the trajectory of an abrasive ball relative to the design helix is constructed. The grooved drum parts are verified through a polishing experiment. The spiral groove of the revolving body is modified and polished. Experiments show that the process not only corrects the shape a spiral groove error, but also reduces the surface roughness of a spiral groove. This study provides a theoretical basis for achieving free-abrasive, tool-free polishing.

Keywords: Revolving body, Spiral groove, Abrasive ball, Active profiling, Modified and polished, Model verification

1 Introduction

Rotary parts with complex spiral grooves are frequently applied to the aerospace, automobile, textile machinery, and petrochemical engineering industries [1, 2]; however, for some closed spiral grooves with complex shapes or structures, the formation and finishing of the parts remain a problem [3, 4]. Superplastic molding, precision casting, additive manufacturing, and other non-mechanical processing for the formation of complex structural parts have significant advantages [5–7]. However, because it is difficult to attain the molding precision required for direct use, the spiral groove formed using these molding methods requires a follow-up finishing to improve the surface quality and accuracy of the shape [7].

Computer-controlled deterministic polishing is the main method used to improve the accuracy of a complex

curved surface shape [8, 9]. This type of polishing mainly applies CNC polishing technology with a small grinding head [10, 11], balloon polishing technology [12–14], magneto-rheological polishing technology [15, 16], ion beam polishing technology [17, 18], and jet polishing technology [19]. Because computer-controlled deterministic polishing is accomplished by controlling the amount of material removed through control of the tool's residence time (or feed rate) at different points on the surface [20–23], surface errors need to be calculated based on the actual surface measurements prior to polishing. Moreover, a quantitative modeling and analysis should be conducted on the material removal when polishing with the aim of controlling the amount of materials removed in an accurate manner. The material removal rates of different points on a work piece surface vary owing to the complexity of the free-form surface, and coupled with the influence of other factors, it is difficult to establish a precise mathematical model. Meanwhile, difficulty also exists in further improving the surface detection precision of the components owing to a limitation of

*Correspondence: fengli001@126.com

² Department of Mechanical Engineering, College of Information & Business, Zhongyuan University of Technology, Zhengzhou 450007, China
Full list of author information is available at the end of the article

the current detection conditions. After generating a dwell function, a 4- or 5-axis numerical control system is generally applied when processing a complex surface. Therefore, polishing technology based on this principle cannot presently be applied to a commercial process [24].

The current complex spiral groove polishing techniques used mainly include manual or semi-manual polishing, the use of a belt, wheel polishing, and electrochemical polishing [25–27]. Among these, manual polishing is inefficient, and the surface processing effect is greatly influenced by the technical level of the workers, the processing consistency is poor, the production environment is harsh, and the health of the operators is impaired [25]. In addition, accessibility to the belt used in grinding wheel polishing for complex inner surfaces is not high, and cannot meet the processing requirements. Moreover, the problem of environmental pollution caused through the use of chemical solutions when applying electrochemical polishing needs to be solved [26].

Free-abrasive polishing, with high process reachability, has significant advantages for the finishing of a complex lumen structure [28–33]. Zhang et al. [34] studied abrasive water jet finishing, and established an abrasive water jet removal model; however, the linear nature of the jet makes it difficult to achieve uniform erosion of all parts of a structured surface, and therefore the formation of good contoured contact and uniform machining results for a structured surface is not possible. Ji et al. [35] proposed a method using a soft milling ball without tool-precision machining, and the impact of soft abrasive flow particles and the particle volume fraction on the grinding effect were studied [28–33]. Zhang Kehua and Ding Jinfu respectively studied the micro-removal force and micro-cutting mechanism. In addition, previous studies have achieved considerable results regarding the cutting modeling and machining of free abrasive particles [33, 36].

In summary, current studies on the finishing of a free-abrasive have mainly focused on improving the surface quality without involving the surface modification. In addition, current studies on the polishing of free-abrasives mainly focused on the movement and control of a single abrasive grain, and research into the different parts has been lacking. The shape and structure of a spiral groove restrict its use as a polishing tool. Therefore, the free-abrasive grain of tool-less finishing is an effective way to improve the surface quality and accuracy of the shape of a non-machined spiral groove. In this paper, the spiral groove of a revolving body is taken as the research object. A method used to make a helical movement of a workpiece, and cut and polish an abrasive grain, is proposed. The principle of the relative motion of the abrasive ball trajectory is studied. The trajectory and design helix are in concordance with a mathematical model. The

grooved drum parts were polished and tested to verify that not only can the error in the shape of the helical groove be corrected but the surface roughness of the helical groove can also be reduced, and the helical groove of the rotating body can be repaired and polished, providing a theoretical basis for free-abrasive tool polishing without a modification.

2 Establishment of Trajectory Control Model for Active Profiling and Polishing

In current free-abrasive machining and computer-controlled polishing, the polishing tool or abrasive particle movement are major aspects, whereas the workpiece is simply used for feed movement or immobility. It can be concluded from the relative movement that the movement of the tool or abrasive particle is active, whereas that of the work piece is passive. Therefore, aiming at achieving rotational spiral parts, in this study, a polishing mode that enables the active movement of the work piece as well as the passive relative movement of the abrasive particles, defined as “active polishing,” was developed, and the concept of “active profiling and polishing” was put forward, which means generating relative movement between abrasive particles and applying a design basis through the movement of the central workpiece, thereby producing a high profile polishing.

In traditional profile polishing, the profiling reference is a polishing tool or abrasive particles, which move along the surface to be machined and remove materials in a uniform manner, achieving a processed surface. As a result, traditional profiling and polishing can only lower the surface roughness instead of improving the accuracy of the shape. In active profiling and polishing, abrasive particles generate relative movement according to the design basis, which marks the profiling for the design basis. Hence, active profiling and polishing can demonstrate a correction of the shape error of the surface to be machined.

In order to realize active polishing, the relative motion between the abrasive ball and spiral groove part needs to meet the following conditions: a spiral relative motion curve consistent with the design basis. Based on the use of a cyclone finisher, adding the upward and downward motion equipment, the rotational parts rotate up and down at the same time, and as a result, the trajectory of the rotational part point has a spiral curve.

Figure 1 demonstrates the principle for active profiling and polishing when rotational parts move in abrasive balls. The rotational parts, which are installed on the abrasive balls in a vertical manner, perform compound motions with a rotational speed of n (r/min) and an axial linear velocity of P (mm/min). Abrasive balls implement reverse rotation with the container and the components

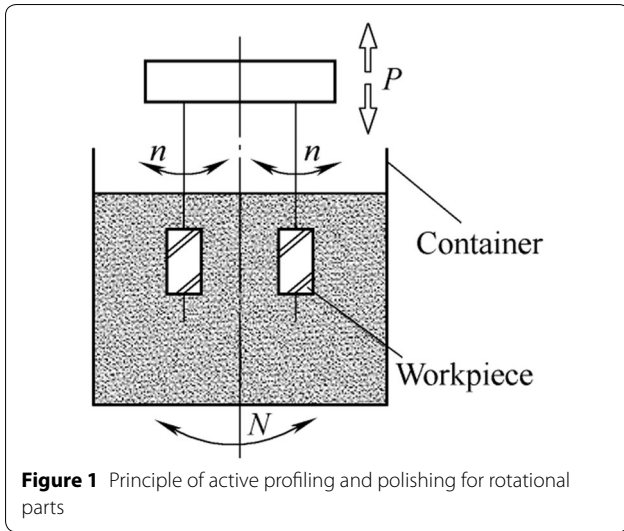


Figure 1 Principle of active profiling and polishing for rotational parts

(at a rotational speed of N r/min), which remain completely submerged in the abrasive balls while in motion. The formation principle of relative motion and spiral curves indicates that the helical curve formed by n and P marks the motion curve of the points on the workpiece surface; relative movements of the surrounding abrasive balls toward the components are $-(n+N)$ (r/min) and $-P$ (mm/min). Hence, the helical curve formed by $-(n+N)$ and $-P$ is the relative movement of the surrounding abrasive balls.

Assuming that $+n$ is the rotational motion of the workpiece, $-N$ will be the rotational motion of the feed cylinder. Thus, the rotational speed and linear velocity synthesis of the abrasive balls relative to the workpiece will be

$$n - (-N) = n + N. \tag{1}$$

When the workpiece rotates at a speed of n , the linear velocity v_1 encircling the work piece will be

$$v_1 = D\pi n. \tag{2}$$

When the roller is conducting a rotation at a speed of N , regardless of the rotation of the abrasive balls, the linear velocity v_2 of the balls tangent to the encircling of the workpiece and rotating with the feed cylinder will be

$$v_2 = 2\pi RN, \tag{3}$$

where R is the radius of gyration of the abrasive balls rotating with the feed cylinder encircling the work piece. In addition,

$$v_1 - (-v_2) = v_1 + v_2. \tag{4}$$

Moreover, the syntheses of the rotating speed and linear velocity are on the same plane.

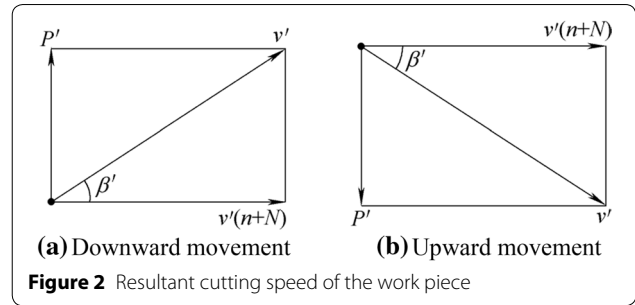


Figure 2 Resultant cutting speed of the work piece

Assuming that P' , $v'(n+N)$, and v' mark the vertical velocity, linear velocity, and resultant velocity of movement of the abrasive balls relative to the encircling of the surface of the workpiece, respectively, when the workpiece conducts downward or upward movement, syntheses of helical motions by the abrasive balls relative to the workpiece are demonstrated, as shown in Figure 2.

In the figures above, $v'(n+N)$ demonstrates the resultant linear velocity of the rotation of the principal axis and feed cylinder in Eqs. (5) and (6). The relative movement between the abrasive balls and workpiece surface is reversed, and is hereby changed into a positive movement for calculation, which means that when $P = -P'$, and $v = -v'$, the following are established:

$$p^2 + (v_1 + v_2)^2 = v^2, \tag{5}$$

$$v = \sqrt{p^2 + (v_1 + v_2)^2}, \tag{6}$$

$$\tan \beta' = p/(v_1 + v_2), \tag{7}$$

$$\beta' = \arctan(p/(v_1 + v_2)). \tag{8}$$

Substituting v_1 and v_2 into Eq. (8), and generating β' , the lead angle of reverse motion by abrasive balls relative to the workpiece is

$$\beta' = \arctan(P/(D\pi n + 2\pi RN)), \tag{9}$$

which indicates the movement relative to the work piece surface formed by the abrasive balls according to a helical curve with a lead angle of β' when the workpiece is moving at a rotational speed of n (r/min) and a linear velocity of P (mm/min).

It can be concluded from Eq. (9) that when D (workpiece parameter), R (mounting parameter), and N (motion parameter of the abrasive balls) are constant, adjusting the speed ratio between n and P can change β' , i.e., the lead angle of the relative motion by the abrasive balls.

If β' can be made consistent with the design curve of a spiral groove on the workpiece surface through an

adjustment, then the abrasive balls will generate a relative helical motion that runs against the curve of a spiral groove on the surface, thereby producing a cutting polish. The design curve of a spiral groove on the workpiece surface is taken as a reference for the relative motion of the abrasive balls. Therefore, not only can the polishing mentioned above reduce the surface roughness of a spiral groove, it can also correct any errors in shape.

Below, D is the diameter of the workpiece, S is the lead of the design curve of a spiral groove on the workpiece surface, and β is the lead angle of the helix, and thus, according to the formula of the lead angle,

$$\beta = \arctan(S/\pi D). \tag{10}$$

Assuming $\beta = \beta'$, namely,

$$\frac{p}{\pi Dn + 2\pi RN} = \frac{S}{\pi D}, \tag{11}$$

$$\frac{S}{p} = 1/\left(n + \frac{2R}{D}\right), \tag{12}$$

where P indicates the axial displacement distance of the workpiece, which is the time it takes for the helical curve to complete one lead, and $n + 2RN/D$ marks the rotational speed of abrasive balls relative to the work piece; in addition, the reciprocal of the rotational speed is the time it takes to complete one rotation. Therefore, Eq. (12) can be interpreted as the time it takes for the workpiece to travel the displacement distance of one lead of the designed helical curve, which is equal for the time required for abrasive balls to rotate one circle relative to the workpiece. This can also be demonstrated as

$$P = \left(n + \frac{2R}{D}N\right)S. \tag{13}$$

This demonstrates the relation model. The model can realize consistency between the spiral trajectory based on the relative motion of the abrasive balls and the design curve under different parameters for rotational parts, with a diameter of D and a surface-designed helical curve lead of S .

Although the relational model in Eq. (13) is established based on the surface helical curve of the rotational parts, when the rotational parts with spiral grooves conduct rotational motion and rectilinear motion at a certain speed, and when the abrasive balls produce a transverse feed movement through extrusion under the function of gravity and then enter the spiral groove at a relatively low speed, it can be considered that a variation of N , the rotational speed of the abrasive balls, is negligible. The lead angle of helical motion is only related to the speed ratio of rotational and linear motion. As a result, the relational

model in Eq. (13) can be applied to the rotational parts with spiral grooves; in other words, it can be used as an active profiling and polishing model for spiral grooved parts of a rotor.

3 Experimental Verification of Active Profiling and Polishing Design of Exoskeleton Arm

3.1 Analysis of Verification Scheme

Different parameters are needed in a polishing experiment for the purpose of verifying the trajectory control model of the active profiling and polishing. In Eq. (13), the maximum value of S is ∞ , under which circumstance of the spiral groove becomes an axial slot, and the relative movement of abrasive balls that runs against the groove can be generated as long as $n=0$, and P is any value other than zero; the minimum value of S is zero, under which circumstance the spiral groove becomes circular, and the relative movement of abrasive balls that runs against the groove can be generated as long as $P=0$, and n is any value other than zero. Hence, there is no need to verify the limit values of S , n , and P . Instead, verification on one typical value will be sufficient. For the sake of the experiment, the aim is to verify one minimum limit value and one typical value of the other parameters.

- (1) Instead of being an independent parameter, R in Eq. (13) is jointly determined based on the installation location of the device and parameter D of the work piece. Changing R and D in a simultaneous manner, the ratio between the two parameters will be constant. As a result, D can be verified as an overall parameter. When $R=0.5D$ marks the minimum value of R/D , the rotational center of the component will be consistent with the center of gyration of the abrasive balls, which is referred to as a concentrically mounted state, as demonstrated in Figure 4. Under such circumstances, Eq. (13) can be expressed as $(N+n)S$.
- (2) In Eq. (13), when $N=0$, namely, when abrasive balls are at rest, $P=nS$.

Therefore, only the minimum values of D and N , and the typical values of all parameters, need to be verified when conducting verification on the trajectory control model of an active profiling and polishing.

3.2 Polishing Equipment

To satisfy the experimental requirements and realize a variation in the parameters, previously developed polishing equipment was employed [37] for verification on a component of a grooved drum. Figure 3 shows the structure of the polishing device used [20, 38], and Table 1

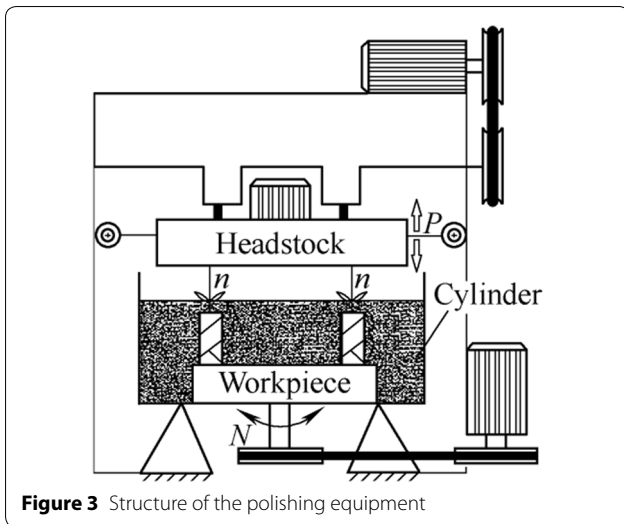


Figure 3 Structure of the polishing equipment

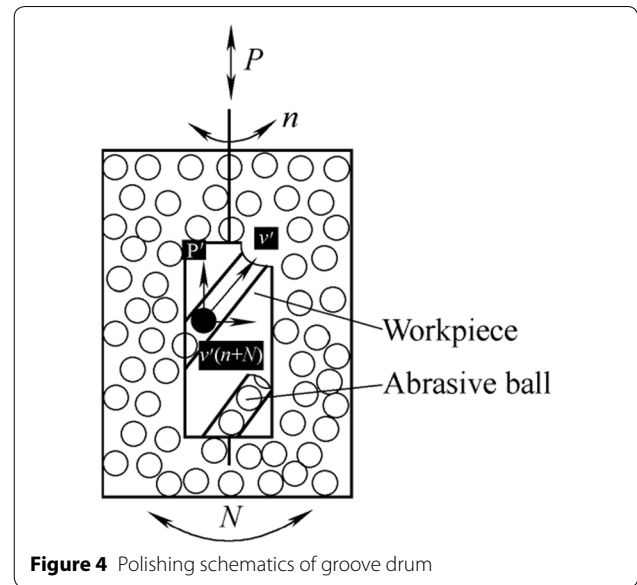


Figure 4 Polishing schematics of groove drum

shows its major parameters. The work piece, which is mounted on the spindle box, can rotate (at a speed of n) under the driving force of the spindle. Meanwhile, it also conducts reciprocating motion (at a speed of P) with the spindle box under the driving force of the crank-link mechanism. Driven by the swing mechanism, the feed cylinder can enable joint rotation (at a speed of N) with inside the medium (abrasive balls). The work piece, which is completely submerged in the medium, can demonstrate linear and rotational motions when the polishing is applied. PLC can control the linear (P) and rotational motions (n) of the workpiece, and a joint rotation (at a speed of N) of the inside medium (abrasive balls).

3.3 Polishing Parts

A grooved drum of a winder was employed as the polishing component in the verification experiment. Figures 4 and 5 [39–41] show a polishing schematic and outline drawing of a superplastic alloy groove drum of a certain size, respectively. The finished grooved drum marks a hollow cylinder, which has a diameter (D) of 82 mm, an aperture (d) of 20 mm, and a length (L) of 176 mm; the depth of the groove in the drum varies from 2.4 to 23 mm, its narrowest width is 5 mm, and its wall thickness is 2.5 mm. In addition, the lead (I) is 152 mm. Direct

molding was applied with pressure. $ZnAl_5$ superplastic alloy marks the material of the components, the mechanical properties of which under normal temperature are as follows: strength of extension of 30–33 kg/mm², yield strength of 27–29 kg/mm², elongation of 5%, and rigidity of HV71.

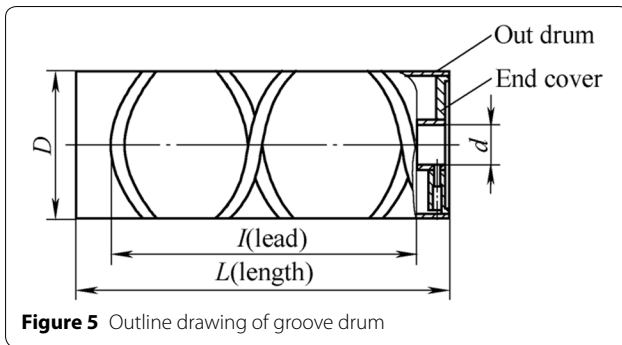
With the typical structure of a rotor spiral groove, the component is equipped with the function of a grooved cylindrical cam. The curve of the groove was designed to be a trade-off between a sinusoid and an exponential curve. The left and right sides of the curve intersect, and a curve connection is employed at the reverse location for a transition, forming a closed cycle. As a result, its groove shape is much more complicated than that of a common rotor spiral groove [21]. Therefore, it is of universal significance for the polishing of a rotor spiral groove to verify the groove drum.

3.4 Calculation of Typical Motion Parameter for Component Polishing

The spiral groove on the periphery of a grooved drum has a trade-off between a sinusoid and an exponential curve. The left and right sides are both closed, and recirculation is conducted. At a location near both ends, the pitch and rotation angle decrease to zero in a gradual manner, and then reverse. The major immediate section is similar to a linear segment on an expanded plane. The pitch and rotational angle remain essentially constant. The error of linear substitution is 7.063% [42]. Therefore, the motion parameter of the immediate section can be approximated through Eq. (13). Specific parameters such as the workpiece parameters (D , S), motion parameters of the

Table 1 Major parameters of the polishing equipment

Cylinder diameter D (mm)	Cylinder height H (mm)	Work-piece, head-stock distance R (mm)	Cylinder rotation speed N (r/min)	Work-piece speed n (r/min)	Workpiece up and down speed P (mm/min)
800	450	150	0–20	0–30	0–10



abrasive balls (N, R), and movement parameters of the workpiece (n) are substituted into Eq. (13) in accordance with the verification scheme, and P is then calculated under different conditions.

3.4.1 Determine the Speed of Workpiece

The value of n is extremely high, and it is difficult for the abrasive balls to enter the spiral groove under centrifugal force. Assuming that the rotational speed of the spindle n is 30 r/min, the lead is 152 mm, the pitch is $152/2=76$ mm, and P is calculated under different conditions:

- (1) When the feed cylinder does not rotate

The abrasive balls are at rest, namely, $N=0$, and thus

$$P = n \times s, P = 30 \times 76 = 2280 \text{ mm/min.}$$

- (2) When the minimum value of D is chosen

Under a concentrically mounted state, $R=0.5D$, and thus $P=(N+n)S$, assuming a rotational speed of the feed cylinder of $N=15$ r/min.

$$P = (30 + 15) \times 76 = 3420 \text{ mm/min.}$$

- (3) When a typical parameter is chosen

Substituting $R=150$ mm and $D=94$ mm into Eq. (13),

$$P = (30 + 2 \times 150/94 \times 15) \times 76 = 5918.1960 \text{ mm/min.}$$

3.4.2 Calculate Frequency of Upward and Downward Movements of the Spindle Box

Here, P is the speed of the upward and downward movements of the axle box, and the pitch per minute is calculated respectively as $2280/76=30$, $3420/76=45$, and $5918.1960/76=77.8710$.

Take the lead of the groove drum as the amplitude of the upward and downward movements of the spindle

box, the amplitude is $2 \times 76=152$ mm. There are two amplitudes in each circulation. As a result, the calculated frequency of the upward and downward movements of the spindle box is 7.5, 11.25, and 19.4678 times/min, respectively.

The calculated motion parameter is entered into the PLC of the equipment, and the polishing experiment is then implemented. The motion syntheses of the transition section of both ends are as follows: n , the rotational speed of the spindle, remains unchanged, and P , the speed of the linear motion by the work piece, gradually decreases to zero. It then becomes negative and conducts a reverse movement. Movement of the work piece is realized through control using the PLC.

3.5 Conditions of Polishing Experiment

In the modeling process, only major factors are taken into consideration, and factors such as the rotation, extrusion, striking of the abrasive ball, and the centrifugal force are simplified in an appropriate manner, the reason for which is that the motion and forces of the abrasive balls when rotating along with the container are relatively complicated. Given the influence of the structure of the spiral groove on the feed movement of the abrasive balls (the mechanism and experiment on the polishing cutting are discussed later), the following items are required when verification on an active profiling and polishing model is conducted using rotor spiral groove parts:

- (1) The diameter of an abrasive ball is significantly lower than the narrowest dimension of the spiral groove.
- (2) An appropriate low-viscosity medium is added to the abrasive balls for cooling and lubrication, reducing the friction and making it possible to assume that the influence of the fluid on the movement of abrasive balls can be neglected.
- (3) When the speed ratio is constant, a lower rotational speed and a linear velocity of the work piece should be applied owing to the low speed of the feed movement generated through extrusion.
- (4) At rotational speed N , the feed cylinder needs to be extremely high to lower the effect of centrifugal force.

Experiment conditions: The surface roughness of the work blank is between Ra 6.3–3.2, carborundum abrasive balls with a diameter of $\varnothing 3$ mm and size of #150 are applied as the polishing medium, clear water is used for the cooling and lubrication. The parameters of the abrasive balls are shown in Table 2.

Table 2 Parameters of the abrasive balls

Hardness HS	Apparent porosity (%)	Bulk density (g/cm ³)	Compressive strength (MPa)	Thermal expansion coefficient (10/ ^o C)	Silicon carbide content (%)	Basic liquid	Consistency (%)
≥ 115	<0.2	>3.10	>2500	4.2	>98	Water	60

Table 3 Number of correct points

Times (min)	5	10	15	20	25	30	35	40	50
Group 1	-	-	-	-	-	30	34	35	36
Group 2	-	-	-	-	30	34	35	36	36
Group 3	-	-	30	34	35	36	36	36	36

3.6 Process and Results of Polishing Experiment

A polishing experiment with three groups of superplastic alloy groove drums of identical size (each group repeated three times) was conducted, and the mean value was recorded. The calculated motion parameters are entered into the PLC for implementation of the polishing experiment. Thirty-six detection points (the distance toward the direction of the extended line is 8.4 mm, and that toward the peripheral direction is 10°) were set in one helical lead with the purpose of detecting the correction efficiency of this polishing method with regard to errors in shape. The ideal coordinate value of each point of the design curve is calculated, and an error of ±0.01 mm is set. During the polishing process, the actual coordinates of each point were measured and compared with the ideal coordinates using a universal tool microscope, and dividing the head by the time interval. If the difference is less than 0.01 mm, the repair can be considered complete. If the 36 test points all meet the requirements, the actual curve can be considered to be in line with the ideal curve, and the error correction of the shape is completed. Table 3 shows the detection of the correct number of points during the polishing process.

In Table 3 and Figure 6, Group 1 demonstrates the state of minimum *N*, Group 2 indicates the state of minimum *R*, and Group 3 indicates the state of the typical parameters.

At 5 and 10 min in Table 3 indicate, a relative surface roughness still exists. Therefore, the coordinates are not determined.

In Group 1, at 30 min, the number of points can be detected, and at 50 min, all points of the actual coordinates satisfy the requirements.

In Group 2, at 25 min, the number of points can be detected, and at 40 min, all points of the actual coordinates satisfy the requirements, and the coordinates tend to be stable.

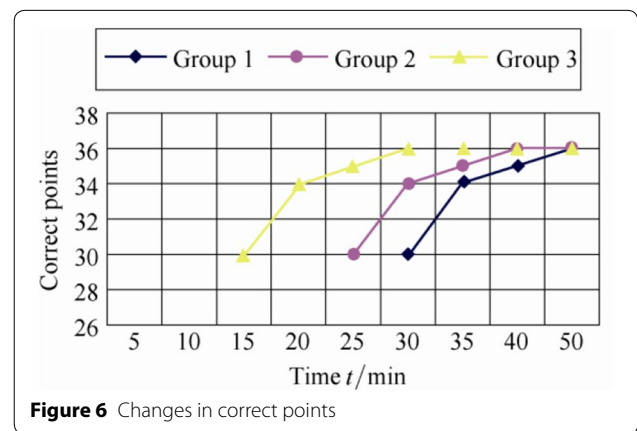


Figure 6 Changes in correct points

In Group 3, at 15 min, the number of points can be detected, and at 30 min, all points of the actual coordinates satisfy the requirements, and the coordinates tend to be stable.

The results indicate that an error in shape can be corrected under the three conditions mentioned above. This indicates that under the conditions in which the model relation is satisfied, regardless of how the parameters are changed, all parameters can realize active polishing, and the mode is reliable.

During the polishing process, it was found that the surface roughness of the spiral groove and the outer surface were not changed much at 5, 10, and 15 min, and the surface roughness was significantly lower than that of the spiral groove at a time of 20 min. The roughness of the spiral groove and the outer surface are basically the same at 50 min, and no longer change. In this case, the *Ra* value was 0.93 μm as determined using a hand-held surface roughness meter. Therefore, it can be determined that the surface roughness value *Ra* of the spiral groove is also 0.93 μm. This indicates that the limit of the surface roughness for the spiral groove polishing under this particular process condition is 0.93 μm.

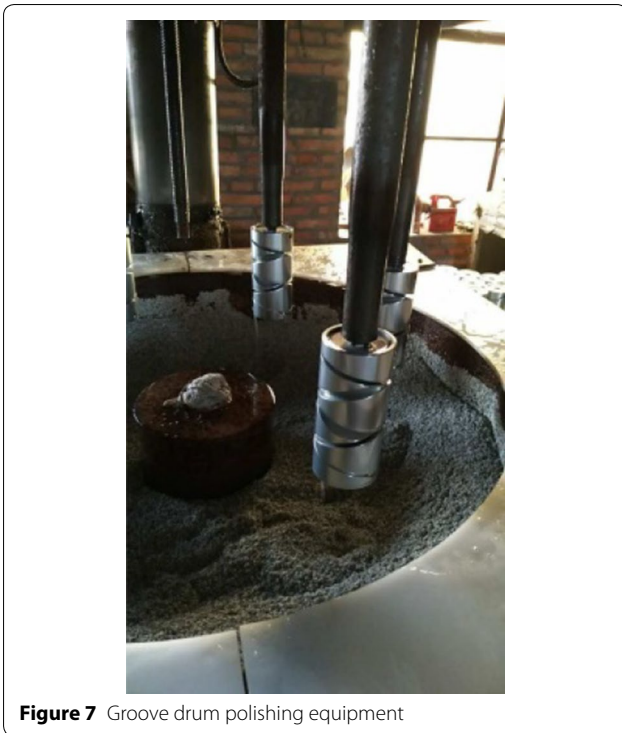


Figure 7 Groove drum polishing equipment

Figure 7 shows the polishing equipment, Figure 8 shows the surface roughness measurement for the polishing of Group 3, and Figures 9 and 10 show a comparison.

4 Conclusions

- (1) Active profiling and polishing is a design basis profiling and polishing, and not only can improve the surface quality, but also the accuracy of the shape. Traditional profiling and polishing sets the surface to be machined on a profile basis. It can only reduce the surface roughness, and is unable to increase shape accuracy.
- (2) The influencing factors and control methods of an abrasive ball relative to the spiral groove movement trajectory are proposed, a consistent mathematical model of abrasive balls relative to the movement trajectory and designed spiral curve is built, and a theoretical basis for the active profiling and polishing of a revolving body with a spiral groove is supplied.
- (3) The spiral groove polishing experiments show that active profiling and polishing can increase the accuracy of the shape and the surface quality of a grooved drum, and has good polishing effectiveness. The problems in which deterministic com-

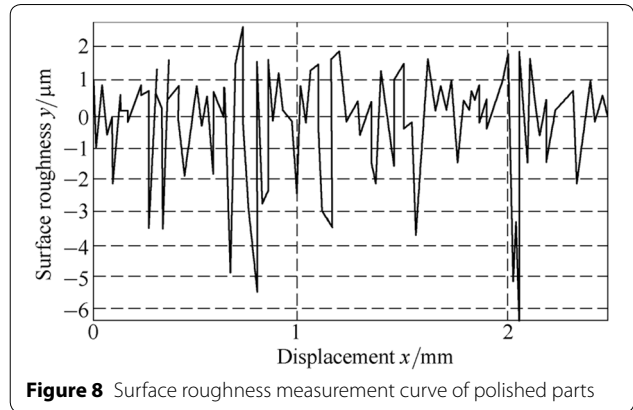


Figure 8 Surface roughness measurement curve of polished parts



Figure 9 Groove drum component of winder prior to polishing

- puter control of the spiral groove polishing is applied, the removal amount is difficult to determine, and a polishing tool is required, are all solved. At the same time, a reference is provided to resolve the free-abrasive tool-less polishing problem.
- (4) A spiral trajectory of the relative movement of an abrasive ball is not only affected by the installation method, installation location, and speed of the revolution, but also by the self rotation, squeeze, impact, and centrifugal force the abrasive ball. The



Figure 10 Groove drum component of winder after polishing

theoretical parameters of the model calculation need to be properly adjusted to achieve the best conditions, and the model needs to be further studied and improved.

Authors' Contributions

GY was in charge of the whole trial; GY and FL wrote the manuscript; GY, FL, Y-MY, S-XZ assisted with sampling and laboratory analyses. All authors read and approved the final manuscript.

Author details

¹ School of Earth Sciences and Resources, China University of Geosciences, Beijing 100083, China. ² Department of Mechanical Engineering, College of Information & Business, Zhongyuan University of Technology, Zhengzhou 450007, China. ³ Electrical and Mechanical College, Zhongyuan University of Technology, Zhengzhou 450007, China. ⁴ Automotive Institute, Henan Mechanical Electrical Secondary School, Zhengzhou 450007, China.

Authors' Information

Guo Yu, born in 1991, is currently a PhD candidate at *China University of Geosciences, China*. His main research direction is precision machining. Tel: +86-13903830850; E-mail: 258550460@qq.com

Feng Li, born in 1981, is currently an associate professor at *College of Information & Business, Zhongyuan University of Technology, China*. He received his master degree on *Mechanical Manufacture and Automation* from *Zhongyuan University of Technology, China*, in 2010. Tel: +86-13526645092; E-mail: fengli001@126.com

Yong-Min Yu, born in 1964, is currently a professor at *Zhongyuan University of Technology, China*. His main research direction is precision machining. Tel: +86-13525529778; E-mail: yym@zut.edu.cn

Shou-Xiang Zai is currently a teacher at *Automotive Institute, Zhongyuan University of Technology, China*. E-mail: 757924495@qq.com

Competing Interests

The authors declare no competing financial interests.

Ethics Approval and Consent to Participate

Not applicable.

Funding

Supported by Key Scientific & Technological Research Project of Henan Province, China (Grant No. 102102210497).

Publisher's Note

Springer Nature remains neutral with regard to jurisdictional claims in published maps and institutional affiliations.

Received: 30 October 2016 Accepted: 16 March 2018

Published online: 23 April 2018

References

- [1] Y C Kuang, F Shu, L M Wu, et al. Numerical simulation method of forming grinding wheel contour for complex spiral curved surfaces. *Journal of Sichuan University (Engineering Science Edition)*, 2013, 45(2): 182–187.
- [2] K Wang, A Q Zang, X W Sun. Study on polishing of screw motor rotors. *Machine Tool & Hydraulics*, 2010, 38(3): 54–56.
- [3] J H Duan, Y Y Shi, J F Zhang, et al. Flexible polishing technology for blade of aviation engine. *Acta Aeronautica et Astronautica Sinica*, 2012, 33(3): 573–578.
- [4] B L Ma, S M Ji, D P Tan. Research of softness abrasive flow machining assisted by chemical polishing. *Light Industry Machinery*, 2014, 32(1): 115–118.
- [5] M Badrossamay, T H C Childs. Further studies in selective laser melting of stainless and tool steel powders. *International Journal of Machine Tools & Manufacture*, 2007, 47(5): 779–784.
- [6] W J Zhu, D C Li, K Ren, et al. Design and test of a practical aircraft model for wind tunnel testing with adjustable control surfaces based on 3D printing. *Acta Aeronautica et Astronautica Sinica*, 2014, 35(2): 400–407. (in Chinese)
- [7] Y M Yu, S X Zai. Analysis on the slotted drum winder with Zn-5Al alloy superplastic forming. *Special Casting and Nonferrous Alloys*, 2014, 34(9): 994–996.
- [8] M J Tai, J F Huang, W L Kao. Robotic polishing of precision molds with uniform material removal control. *International Journal of Machine Tools & Manufacture*, 2009, 49: 885–895.
- [9] J L Yuan, Z Wu, B H Lv, et al. Review on ultra-precision polishing technology of aspheric surface. *Journal of Mechanical Engineering*, 2012, 48(23): 167–177. (in Chinese)
- [10] R A Jones. Optimization of computer controlled polishing. *APP. OPT.*, 1977, 16(1): 218–224.
- [11] G L Wu, Y F Dai, S Y Li. Research on the determination for the abrasive disk's dimension in aspheric optics machining. *Journal of Mechanical Engineering*, 2004, 40(1): 147–150. (in Chinese)
- [12] R G Bingham, D D Walker, D L King, et al. A novel automated process for aspheric surfaces. *Current Developments in Lens Design and Optical Systems Engineering*, August 2–4, 2000, San Diego, CA, United states. Bellingham: SPIE, 2000: 445–450.
- [13] D D Walker, D Brooks, A King, et al. The "precession" tooling for Polishing and figuring flat, spherical and as pheric surfaces. *Optics Express*, 2003, 11(8): 958–964.
- [14] W Zhang, H Y Li, H Jin. Research on digital simulation and experiment of removal function of bonnet tool Polishing. *Journal of Mechanical Engineering*, 2009, 45(2): 308–312. (in Chinese)
- [15] F Zhang, J C Yu, X J Zhang, et al. Magneto rheological finishing technology. *Optics and Precision Engineering*, 1999, 7(5): 1–8.
- [16] X Q Peng, Y F Dai, S Y Li. Material removal model of magneto rheological finishing. *Journal of Mechanical Engineering*, 2004, 40(4): 67–70. (in Chinese)

- [17] X H Xie, Y Hao, L Zhou, et al. High thermal expansion optical component machined by ion beam figuring. *Optical Engineering*, 2012, 51(1): 13401–13401–8.
- [18] C J Jiao, S Y Li, D F Wang, et al. Material removal property in ion figuring process for optical components. *Optics and Precision Engineering*, 2007, 15(10): 1520–1526.
- [19] P J Guo, H Fang, J C Yu. Research on material removal mechanism of fluid jet polishing. *Laser Journal*, 2008, 29(1): 25–27.
- [20] A J Robert. Optimization of computer controlled polishing. *Applied Optics*, 1977, 16(1): 218–224.
- [21] C Song, Y F Dai, X Q Xiao. Model and algorithm based on accurate realization of dwell time in magnetorheological finishing. *Applied Optics*, 2010, 49(19): 3676–3683.
- [22] H B Cheng, Z G Feng, K Cheng, et al. Design of a six-axis high precision machine tool and its application in machining aspherical optical mirrors. *International Journal of Machine Tools & Manufacture*, 2005, 45: 1085–1094.
- [23] A Ronald, M Ralph, R N Francis. Computer assisted optical surfacing. *Applied Optics*, 1972, 11(12): 2739–2747.
- [24] S M Ji, X S Du, G D Cheng, et al. Review on deterministic polishing. *Aviation Precision Manufacturing Technology*, 2010, 46(6): 1–12.
- [25] B Rosa, P Mognol, J Hascoet. Laser polishing of additive laser manufacturing surfaces. *Journal of Laser Applications*, 2015, 27(S2): S29102.
- [26] E Lyczkowska, P Szymczyk, B Dybala, et al. Chemical polishing of scaffolds made of Ti–6Al–7Nb alloy by additive manufacturing. *Archives of Civil & Mechanical Engineering*, 2014, 1(4): 586–594.
- [27] G J Xiao, Y Huang, H Yi. Experimental research of new belt grinding method for consistency of blisk profile and surface precision. *Acta Aeronautica et Astronautica Sinica*, 2016, 37(5): 1666–1676. (in Chinese)
- [28] S Singh, A S A Raj, M R Sankar, et al. Finishing force analysis and simulation of nanosurface roughness in abrasive flow finishing process using medium rheological properties. *The International Journal of Advanced Manufacturing Technology*, 2016, 85(9): 2163–2178.
- [29] T S Kavithaa, N Balashanmugam. Nanometric surface finishing of typical industrial components by abrasive flow finishing. *The International Journal of Advanced Manufacturing Technology*, 2016, 85(9): 1–8.
- [30] S M Ji, C Li, D P Tan, et al. Study on machinability of softness abrasive flow based on preston equation. *Journal of Mechanical Engineering*, 2011, 47(17): 156–163. (in Chinese)
- [31] J Y Li, Y Xu, L F Yang, et al. Research on abrasive flow machining experiments of non-linear tubes. *China Mechanical Engineering*, 2014, 25(13): 1729–1734. (in Chinese)
- [32] Y Z Fu, X P Wang, H Gao, et al. Blade surface uniformity of blisk finished by abrasive flow machining. *The International Journal of Advanced Manufacturing Technology*, 2016, 84(5): 1725–1735.
- [33] H Gao, M Y Wu, Y Z Fu, et al. Development of theory and technology in fluid abrasive finishing technology. *Journal of Mechanical Engineering*, 2015, 51(7): 174–187. (in Chinese)
- [34] C G Zhang, Y Zhang, F H Zhang, et al. Study on removal model of abrasive waterjet machining. *Journal of Mechanical Engineering*, 2015, 51(7): 188–196. (in Chinese)
- [35] S M Ji, S C Zhang, X Zhang, et al. Surface finishing methods based on the constraint hydraulic abrasive flow field: China, 10067628.3. 2007–03–21.
- [36] H Gao, S C Li, Y Z Fu, et al. Study of abrasive flow machining of additively manufactured metal grilling. *Acta Aeronautica et Astronautica Sinica*, 2017, 38(10): 421210–421210
- [37] Y L Liu, W Hong, J Hang, et al. Parametric design and simulation of swirl polishing machine. *Light Industry Science and Technology*, 2016(11): 57–59.
- [38] Y M Yu, F Li. Development of active copying polishing machine for metal grooved drum spiral groove. *Manufacturing Technology & Machine Tool*, 2014, 7: 98–101.
- [39] J C Yang. Study on the thread guide trench curved surface of a grooved drum. *Journal of Textile Research*, 2006, 27(3): 4–7.
- [40] Y Lv. Metal grooved drum processed by superplastic technology. *Textile Machinery*, 1994(5): 13–14.
- [41] Y M Yu, S X Zai. Study on the polishing process of super-plastic aluminum alloy grooved drum. *Wool Textile Journal*, 2014, 42(6): 39–42.
- [42] Y Q Jia, P X Wang. Numerically controlled milling helical flute of bobbin winder's fluted roller and milling cutter's design. *Journal of Taiyuan Heavy Machinery Institute*, 1995, 16(1): 1–7.

Submit your manuscript to a SpringerOpen® journal and benefit from:

- Convenient online submission
- Rigorous peer review
- Open access: articles freely available online
- High visibility within the field
- Retaining the copyright to your article

Submit your next manuscript at ► springeropen.com
